



# Facile synthesis of hollow bioactive glass nanospheres with tunable size



Tao Liu<sup>a,b,\*</sup>, Zhihui Li<sup>a</sup>, Xinbo Ding<sup>a,\*</sup>, Lixiang Zhang<sup>a</sup>, Yuanxing Zi<sup>a</sup>

<sup>a</sup> College of Materials and Textiles, Zhejiang Sci-Tech University, Hangzhou 310018, China

<sup>b</sup> Keyi College, Zhejiang Sci-Tech University, Hangzhou 311121, China

## ARTICLE INFO

### Article history:

Received 19 October 2016

Received in revised form 16 December 2016

Accepted 30 December 2016

Available online 31 December 2016

### Keywords:

Bioactive glass

Hollow nanospheres

Sol-gel method

Bioactivity

## ABSTRACT

Hollow nanospherical bioactive glasses were conducted through sol-gel process using poly(acrylic acid) (PAA) as the template. The incorporation of PAA was to form the core after air combustion, whereas the inorganic shell was produced by glass precursor. The mixture of different tetraorthosilicate (TEOS)/PAA contents into a glass network tailored the shell thickness, morphological, and structural properties of HBGs. The *in vitro* bioactivity evaluation confirmed that HBG2 sample exhibited good apatite formation ability, thereby denoting that the proposed method enhanced the potential application of HBGs in bone tissue regeneration and drug delivery.

© 2017 Elsevier B.V. All rights reserved.

## 1. Introduction

The invention of bioactive glasses (BGs) has brought a new therapeutic revolution in bone implantation on account of their reaction products to strongly integrate with live bone. This feature of BGs has inspired the rapid development of synthetic strategy toward the structure and texture of these bioactive materials. Sol-gel method is mostly used route compared with traditional melt-quenching for the synthesis of BGs. Sol-gel derived BGs in the CaO-SiO<sub>2</sub>-P<sub>2</sub>O<sub>5</sub> system show large porosity, high surface area, and high purity, all of which result in superior biological properties (i.e., bioactivity, restorability, and osteoconductivity) compared with the conventional melt-quenched BGs [1–3]. In addition, these sol-gel BGs can be produced after relatively low temperatures, thus allowing the incorporation of biologically active agents. In the sense, BGs in the form of spherical particles and hollow structure have been suggested as the appropriate delivery carrier. Moreover, due to their low density, large specific surface area, and high storage capacity, these hollow BG (HBG) spheres receive considerable attention for catalysis, separation and drug delivery [4–6].

Generally, polymer template method was reported to fabricate such hollow matrix. Papas et al. synthesized the hollow BG nanospheres in the sub-micron size range using polystyrene (PS) nanospheres as the template [4]. Li et al. also reported the HBG nanospheres with the incorporation of monodispersed PS templates and cetyltrimethylammonium bromide [6]. However, PS

templates with a uniform size distribution were the necessary precondition for the hollow structure. In this regard, we developed a facile and one-step method to prepare HBGs through directly introducing PAA as the sacrificial template. The PAA template as the cores is to support for the information and further growth of the stable primary inorganic network as the shells, thereby producing the core-shell structure of PAA@BG (Fig. 1). The surface morphology and size of HBG nanospheres could be controlled by the weight ratio of TEOS/PAA. Furthermore, the bioactivity of the obtained materials was subsequently investigated in simulated body fluid (SBF) solution.

## 2. Experimental introduction

### 2.1. Synthesis

The HBGs with tunable sizes were synthesized by adding different weight ratio of TEOS/PAA (Table 1). Typically, 0.2 g of PAA (oligomer: Mw ~ 3000), and 4.5 mL of ammonium hydroxide (NH<sub>4</sub>OH 33%) were dissolved in 90 mL of ethanol at room temperature until the mixture became clear. Accordingly, TEOS, triethylphosphate (TEP), and calcium nitrate (Ca(NO<sub>3</sub>)<sub>2</sub>·4H<sub>2</sub>O, CaNT) system were added in every 1 h interval to react completely. The above mixture was continuously stirred for 72 h for complete hydrolysis. The obtained precipitates were separated by centrifugation and washed with ethanol and water, followed by drying at 75 °C. The dried powders were further calcined at 550 °C for 10 h in air. For *in vitro* bioactivity test, the bioactivity of HBG2 materials were assessed by soaking in SBF at 37 °C for 1, 3, and 7 days [7].

\* Corresponding authors at: College of Materials and Textiles, Zhejiang Sci-Tech University, Hangzhou 310018, China (T. Liu and X. Ding).

E-mail addresses: [maggie\\_liu310@163.com](mailto:maggie_liu310@163.com) (T. Liu), [dxblt@zstu.edu.cn](mailto:dxblt@zstu.edu.cn) (X. Ding).

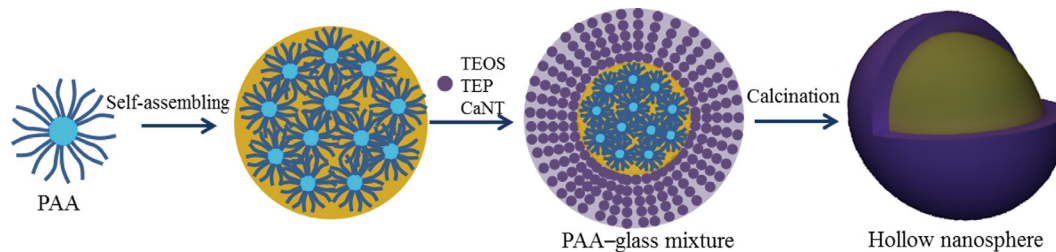


Fig. 1. Illustration of formation mechanism of HBG spheres.

**Table 1**  
Chemical compositions and structural parameters of HBGs.

Sample	PAA/g <sup>a</sup>	TEOS/g	TEP/g	CaNT/g	Surface area/m <sup>2</sup> g <sup>-1</sup>	Pore volume/cm <sup>3</sup> g <sup>-1</sup>	Pore size/nm
HBG1	0.20	0.90	0.20	0.13	50.16	0.129	10.3
HBG2	0.20	1.80	0.39	0.26	41.58	0.101	10.19
HBG3	0.20	2.70	0.59	0.38	40.88	0.079	9.42
HBG4	0.20	3.60	0.79	0.51	33.89	0.072	9.76

<sup>a</sup> For comparison, the template PAA content was kept fixed at constant value.

## 2.2. Characterization

The obtained HBGs were characterized by field-emission scanning electron microscopy (FESEM; Ultra-55, Carl Zeiss) with Energy dispersive spectrometer (EDS), and fourier transitioned infrared spectroscopy (FTIR; Nicolet 5700, Nicolet USA). Transmission electron microscopy (TEM) images were obtained on JEOL JEM2100. The particle size distribution was determined by dynamic light scattering measurements (Zetasizer Nano S, Malvern). Powder X-ray diffraction (XRD) patterns were recorded on Philips PW-1050 diffractometer with Ni-filtered CuK $\alpha$  radiation. Nitrogen adsorption and desorption isotherms were measured on Micromeritics ASAP 2020 system.

## 3. Results and discussion

It should be mentioned that the particle size of the as-synthesized nanoparticles can be tailored by these experimental parameters such as the BG sol composition and processing parameters (e.g., pH value of sol, hydrolysis temperature, aging time, and template molecular weight) [8]. Herein the key parameters, the weight ratios of TEOS/PAA, are easily tuned by changing TEOS contents while PAA parameters kept unchanged. Fig. 2 shows the FESEM and TEM images of the HBGs with different sizes. All the samples (Fig. 2a) displayed a spherical shape in morphology, while the hollow structure in TEM analysis (Fig. 2b) was observed after the complete removal of the template. For HBG2 and HBG3 samples, the hollow structure of these nanospheres would be well distinguished by the broken particles (the yellow arrow). The particle sizes for HBG1, HBG2, HBG3, and HBG4 nanospheres were  $81.0 \pm 15.6$ ,  $92.0 \pm 14.7$ ,  $109.9 \pm 21.3$ , and  $133.3 \pm 25.6$  nm, respectively (Fig. 2c). The addition of TEOS contents in the matrix increased the shell thickness of these as-prepared HBG samples, thereby indirectly broadening the size distribution of HBG nanospheres. These observations occurred in shell thickness could be further verified by TEM analysis. In Fig. 2b, almost all the particles showed a spherical morphology with a hollow core. At the high TEOS content, the size distribution and the shell thickness of HBG4 sample became broad, consistent with the FESEM observation.

The data obtained from surface area nitrogen analysis on adsorption/desorption curves are listed in Table 1. Basically, the

isotherm of these samples after the calcination, shows a hysteresis loop on the desorption branch which is Type IV, characteristic for mesoporous materials (Fig. S1). For HBG1 sample, the relative high specific area compared with other similar structures was due to the thin shell thickness. The specific surface area of our HBGs was much higher than the reported HBG microsphere in the literature [4,6]. Also, the total pore volume of the obtained samples calculated at 0.99 of the relative pressure decreased from 0.129 to  $0.072 \text{ cm}^3/\text{g}$ .

The representative HBG2 material was selected for bioactivity assessment. Fig. 3a shows the FESEM micrographs of HBG2 material after soaking in SBF at 37 °C for 1, 3, and 7 days. After 1d in SBF, the surface of HBG2 sample became rougher than that of the untreated sample. After 3d in SBF, HBG2 sample had a thin layer composed of several cluster-like apatite crystallites on the surface. With increasing soaking time, numerous apatite clusters were formed on the surface as compared with that after soaking for 3d. The corresponding EDS spectra (Fig. 3b) also demonstrated that the increase in phosphorous and calcium content, which suggested the formation of bone-like hydroxyapatite (HA). Meanwhile, the XRD pattern showed the structural changes that occurred with an increase in immersion time (Fig. 3c). The HBG2 nanoparticles before soaking in SBF exhibited amorphous nature of the silica network with a broad diffraction peak between  $20^\circ$  and  $24^\circ/2\theta$ . After 1d in SBF, two diffraction peaks at  $26^\circ$  and  $32^\circ/2\theta$  emerged, corresponding to the apatite (002) and (211) reflections (JCPDS# 09-0432), respectively [8,9]. Besides, the main diffraction peaks (002) and (211) of the sample became narrower with increasing soaking time, along with the new strong peaks at  $45^\circ/2\theta$  (113). The XRD patterns as a function of soaking time indicated that the evolution of HA crystals in SBF. Fig. 3d shows the FTIR spectra of HBGs before and after soaking in SBF. The bending and stretching vibrations of Si–O–Si bands were detected at around 1090, 802, and  $469 \text{ cm}^{-1}$ . After soaking, two obvious bands at 606 and  $567 \text{ cm}^{-1}$  appeared, associating with the crystalline O–P–O vibrational bands. The result indicated an apatite-like phase formation [10,11]. The weak vibrational peaks at 1470, 1410 and  $903 \text{ cm}^{-1}$  in the sample after 7d SBF were associated with the C–O bending mode, suggesting a carbonated HA characteristic [12]. The interesting vibrational band intensity at 606 and  $567 \text{ cm}^{-1}$  increased with prolonging immersion time, confirming that an expected HA nanoparticle formation, which was consistent with the EDS and WAXRD results.

Download English Version:

<https://daneshyari.com/en/article/5464181>

Download Persian Version:

<https://daneshyari.com/article/5464181>

[Daneshyari.com](https://daneshyari.com)